Phase-slip-like resistivity in underdoped $YBa_2Cu_3O_7$

M. M. Abdelhadi* and J. A. Jung†

Department of Physics, University of Alberta, Edmonton, Alberta, Canada T6G 2J1

(Received 31 May 2002; revised manuscript received 4 November 2002; published 6 February 2003)

We investigated the anomalous peak resistivity below the onset T_c in underdoped $YBa_2Cu_3O_7$, reminiscent of that observed in one-dimensional (1D) wires of conventional superconductors. We performed measurements of the angular dependence of resistivity $\rho(\theta)$ in a magnetic field and the temperature dependence of resistivity $\rho(T)$, which exhibit a peak for $\mathbf{B}\| ab$ planes. This peak in $\rho(T)$ disappears for $\mathbf{B}\| c$ axis. The width of the corresponding maximum in $\rho(\theta)$ at $\theta=0°$ ($\mathbf{B}\| ab$ planes) decreases with the increasing c-axis component of the field ($B \sin\theta$). The maximum in $\rho(\theta)$ and $\rho(T)$ decreases with an increasing applied transport current. We analyzed the data using three different models of resistivity based on a 2D resistor array, flux motion, and thermally activated phase slips. Numerical calculations suggest that in a filamentary underdoped system, the phase-slip events could produce an anomalous resistivity close to T_c.

DOI: 10.1103/PhysRevB.67.054502 PACS number(s): 74.78.−w, 74.40.+k, 74.72.Bk

I. INTRODUCTION

Observation of a large resistive peak in the temperature dependence of resistivity $\rho(T)$ just below the onset T_c has been reported in crystals of high-T_c superconductors (HTSCs) like $(\mathrm{Nd,Pr})_{1.85}\mathrm{Ce}_{0.15}\mathrm{CuO}_{4-y}$,[1] YBCO(123),[2] and $Bi_2Sr_2CaCu_2O_8$ [BSCCO(2212)].[3] In all these cases, the magnitude of the resistive peak is higher than the resistivity at the onset T_c. The peak shows an anomalous behavior in a magnetic field applied along the c axis. Its magnitude decreases with an increasing field, and in high enough fields the peak is completely suppressed. The applied transport current has the same effect on the peak, i.e., the peak's magnitude decreases with an increasing applied current.

These phenomena are of considerable interest because of their striking qualitative similarity to those observed in conventional superconductors (LTSCs) like superconducting mesoscopic Al wires,[4,5] thin films of Al,[6,7] (NbV)N, NbV, VN, (NbTi)N,[8] and disordered metallic glasses of $Zr_{60}Cu_{60}$.[9] Mosqueira *et al.*[2] reported the resistive anomalous peak in $\rho_{ab}(T)$ of YBCO crystals of $T_c(R=0)=89$ K. This anomaly was eliminated by successive annealing of the sample in oxygen. This annealing also led to an increase of $T_c(R=0)$ up to 90.3 K (close to the optimal doping). The authors concluded that the peak could be related to very small T_c inhomogeneities nonuniformly distributed in the crystal. They performed computer simulations of the temperature dependence of the anomalous resistivity using the model of a two-dimensional electric circuit: an array of resistors whose resistivity depends on temperature. The nonuniformly distributed T_c inhomogeneities were introduced by assuming that these resistors have different (higher or lower) T_c. The authors stated that the uniformly distributed T_c inhomogeneities at large length scales broaden the resistive transition only, and do not produce a peak. A similar approach was introduced earlier by Vaglio *et al.*[8] to explain the resistance-peak anomaly in non-homogeneous thin films of (NbV)N, NbN, VN, and (NbTi)N. They concluded that "the current redistribution" caused by the sample's inhomogeneity, is responsible for the observed phenomena.

Current redistribution effects in an inhomogeneous sample were also considered by Nordstrom and Rapp[9] in their interpretation of the resistive peak anomaly in superconducting amorphous thick films of $Zr_{60}Cu_{40}$. Kwong *et al.*[6] observed an anomalous peak in the resistive transition of a two-dimensional (2D) 25-nm-thick aluminum film containing regions of different but comparable, transition temperatures. Disordered regions of lower T_c were produced by the reactive-ion etching process. Their observation seems to support earlier interpretations based on T_c inhomogeneities and current redistribution effects. The authors stated, however, that the anomaly could originate from a discontinuity of the superconducting potential at the normal-superconducting metal (N-S) interface, and for superconducting electrodes placed sufficiently close to the interface, this potential exceeds the normal-state value. Spahn and Keck[7] found that the anomaly appears in 2D Al films with a thickness between 13 and 40 nm. They argued that this effect could be caused by an interaction between the superconducting fluctuations and the conduction electrons.

Extensive studies of the resistive anomaly were also performed on 1D Al strips with a width less than the coherence length and the magnetic penetration depth, by Santhanam *et al.*[4] and Moshchalkov *et al.*[5] Santhanam *et al.* argued that the Al wire could be treated (at temperatures close to T_c) as a coherent region comprising normal (N) and superconducting (S) phases. The resulting N-S interface gives rise to a quasiparticle charge imbalance induced by the bias current, and consequently to the observed changes in resistivity. Moshchalkov *et al.* performed quantitative analysis of the anomaly using Langer-Ambegaokar (LA) (Ref. 10) and McCumber-Halperin (MH) (Ref. 11) models of the thermally activated phase-slips of the superconducting order parameter. LA-MH models were adopted with the modification which assumes that in quasi-1D superconducting wires the normal current and the supercurrent can only flow in series, and the total resistance is the sum of the normal resistance R_N and the phase-slip resistance R_S. Good quantitative agreement between the experimental data and the calculated resistance $R(T)$ was obtained.

Crusellas *et al.*[1] and Han *et al.*[3] proposed that the anomaly in $\rho_{ab}(T)$ of $(\mathrm{Pr,Nd})_{1.85}\mathrm{Ce}_{0.15}\mathrm{CuO}_{4-y}$ and

BSCCO(2212) crystals is the manifestation of a quasireentrant behavior, which results from the intrinsic granularity. Han *et al.* rejected the explanation based on non-uniformly distributed T_c inhomogeneities (Ref. 2), because of the observation of an anomalous peak in the I-V characteristics, which were measured at different magnetic fields. However, Crusellas *et al.*[1] stated that the anomaly is strongly influenced by the distribution of defects, after it was observed that high temperature annealing reduces the size of the resistive anomaly in $(\mathrm{Pr,Nd})_{1.85}\mathrm{Ce}_{0.15}\mathrm{CuO}_{4-y}$ crystals.

Briefly, the interpretation of the anomalous resistive peaks in HTSCs concentrates on two possible sources of this effect: nonuniformly distributed T_c inhomogeneities and intrinsic granularity. The explanation of the anomalous resistivity in LTSC films took into account the effects of T_c-inhomogeneities (and related current redistribution), N-S interfaces, and the interaction between superconducting fluctuations and the conduction electrons. It was also suggested that the anomaly in 1D LTSC (Al) strips (wires) originates from the presence of N-S interfaces and/or thermally activated phase-slips of the order parameter. These various interpretations are the source of a number of unanswered questions.

(1) According to Browning *et al.*[12] in YBCO single crystals of $T_c = 93$ K and a transition width of $\Delta T_c = 0.2$ K, a large variation in the oxygen content $7-\delta$ can occur across the sample as revealed by high resolution scanning x-ray diffractometry (which was performed using a 10-μm-wide x-ray beam). $7-\delta$ in these crystals ranges between 6.80 and 7.00, which corresponds to a change of T_c by about 10 K. In spite of these nonuniform T_c inhomogeneities, the crystals have small resistivities ($\rho \simeq 40\ \mu\Omega$ cm at 100 K) and do not show any resistive peak anomalies at the onset T_c in $\rho(T)$. These results throw doubt on whether the 2D resistive model alone (as proposed in Ref. 2 for YBCO) can explain the observed anomalies.

(2) The resistive anomalies observed in LTSC films and wires (strips) are similar, and their interpretation suggests the link between the presence of inhomogeneities (T_c-inhomogeneities, N-S interfaces) and the superconducting fluctuations, including phase slips of the order parameter. Could this explanation be also applied to HTSCs?

(3) Moshchalkov *et al.*[5] introduced the phase slip resistivity (according to the 1D LA-MH model[10,11]) combined with the normal state resistivity in order to explain the anomalous resistive peak in 1D aluminum wires. Experiments by Browning *et al.* [see (1)] suggest filamentary phase separation and filamentary flow of the current in some YBCO crystals with sharp superconducting transitions, which do not show resistive anomalies. Does this mean, using the analogy to LTSCs, that the presence of nonuniformly distributed inhomogeneities in HTSCs is the necessary but not sufficient condition to observe the resistive anomaly? What is the other condition? Could this be a 1D current flow in an inhomogeneous system?

(4) What is the contribution of the magnetic flux motion (pinning) to the observed resistive anomalies in HTSCs?

In order to answer these questions new experiments are needed. We decided to perform measurements of the angular dependence of resistivity in a magnetic field. This decision was stimulated by the experiments done on $\mathrm{Pr}_{1.85}\mathrm{Ce}_{0.15}\mathrm{Cu}_{4-y}$ crystals,[1] in which the resistive anomaly was investigated for two different directions of the applied magnetic field, namely, along the c axis and along the ab planes. The effect of the magnetic field on the anomaly was completely different for these two orientations. Taking into account the fact that the presence of the nonuniform T_c inhomogeneities is a necessary but not sufficient condition to observe the resistive anomalies, we investigated the temperature dependence of resistivity on a large number of YBCO samples. We decided to study YBCO thin films, both optimally doped and underdoped, because they are readily accessible from different research groups and can be deposited on various substrates using several different deposition techniques. The bridges for the resistive measurements can be made relatively easily on thin films using standard photolithographic techniques. The resistive peak anomaly and the reduction of its magnitude with an increasing magnetic field and an increasing applied current, were observed in an underdoped film after investigation of 15 YBCO films of T_c ranging between 79 and 90.5 K. This film was then used to perform detailed measurements of the angular dependence of resistivity in a magnetic field. The resulting experimental data were analyzed using three different models: a two-dimensional resistor model, a magnetic flux motion model, and the LA-MH thermally activated phase-slip theory.

II. EXPERIMENTAL PROCEDURE

A. Sample preparation

C-axis oriented YBCO thin films were prepared using off-axis rf magnetron sputtering and laser ablation from stoichiometric $\mathrm{YBa_2Cu_3O_{7-\delta}}$ targets of 99.999% purity. Films were deposited on three different types of substrates: $\mathrm{SrTiO_3}$, $\mathrm{LaAlO_3}$, and sapphire (with a $\mathrm{CeO_2}$ buffer layer).

We investigated 15 YBCO thin films (both underdoped and close to the optimal doping) of various zero-resistance transition temperatures (between 79 and 90.5 K) and thicknesses (between 100 and 600 nm). YBCO films were patterned, using conventional photolithography and wet etching technique, into a form of a 30–60-μm wide and 6.4-mm-long strips with six measurement probes. Large area silver contacts were deposited on the film by rf magnetron sputtering in order to minimize Joule heating. Copper leads were attached to silver contacts using mechanically pressed indium. The distance between voltage probes was 0.4 mm.

The anomalous resistivity was observed in an underdoped YBCO thin film. This film (140 nm thick), was deposited on a (1000)-oriented sapphire substrate (with a $\mathrm{CeO_2}$ buffer layer) using laser ablation technique. X-ray diffraction (XRD) data of this film showed the pattern of a characteristic stoichiometric c axis oriented YBCO film. The data did not reveal any impurity phases. The XRD data gave a c-axis lattice spacing of 11.70 Å, which corresponds to an oxygen content of about 6.8 and $T_c(R=0)$ of about 80 K.[13]

The sample exhibits a vanishing zero-field resistivity at $T_c = 81.7$ K and has a room temperature resistivity $\rho_{300K} = 34.2\ \mu\Omega$ cm ($\rho_{300K}/\rho_{100K} = 2.4$). The resistivity of this underdoped YBCO film is lower than that expected for optimally doped YBCO. Normally removing oxygen from optimally doped YBCO decreases T_c and increases the normal state resistivity, and vice versa, adding oxygen to an underdoped YBCO, increases T_c and decreases the resistivity, with the lowest resistivity expected for optimally doped samples. However, at a fixed level of oxygen doping, different samples may have lower or higher resistivities depending on the distribution of chain oxygen O(1) and interchain oxygen O(5) in the chain-layers. Our recent results[14] obtained on underdoped YBCO films (with $T_c \simeq 84$–85 K) revealed that annealing of samples in argon at 400 K (120 °C) increases both T_c and resistivity [This annealing also transforms a nonlinear temperature dependence of resistivity (with a flattening below 200 K) into a linear dependence.] Annealing YBCO at 400 K in argon causes a redistribution of oxygen in the chain layers without affecting the overall concentration of oxygen in the sample.[15] The resistivity of a twinned YBCO film can be considered as the effective resistivity of the parallel combination of the plane and chain-layer resistivities. Even optimally doped samples that were well annealed in oxygen, still contain a few percent of interchain oxygen O(5).[15,16] In slightly underdoped samples, the presence of interchain oxygen O(5) located between not fully occupied chains could force the transport current in the chain layer to flow along a path of the lowest resistance, i.e., to zigzag between the chains via the occupied O(5) sites. An increase of T_c and the resistivity upon annealing at 400 K could then result from a thermally activated diffusion of some O(5) oxygen into empty O(1) chain sites. During this process the chain layer could lose some of the interchain low resistance links. We therefore believe that low resistivity observed in the underdoped film could be a consequence of a chain-layer conductivity being enhanced by the presence of interchain links. These links could be formed by O(5) oxygen during fast cooling of the film down from high deposition temperature.

B. Measurement procedure

The investigation of the resistive anomalies was based on the following measurements: (a) the measurement of the temperature dependence of resistivity $\rho(T)$ between room temperature and $T_c(R=0)$ in a zero magnetic field; (b) the measurement of the temperature dependence of resistivity $\rho(T)$ between the onset T_c and $T_c(R=0)$ in an external magnetic field applied either parallel or perpendicular to the *ab* planes; (c) the measurement of the angular dependence of resistivity $\rho(\theta)$ as a function of the angle θ between the *ab* planes and the direction of the fixed applied magnetic field at fixed temperatures between the onset T_c and $T_c(R=0)$; and (d) the measurement of $\rho(\theta)$ as a function of the magnitude of the magnetic field **B** and the applied transport current density **J**. The angular measurements were performed by rotating a copper sample holder about its vertical axis in a horizontal magnetic field up to 1 T, using a combination of a step motor and backlash-free gear reducer. The angle was accurately monitored by an 8000-line optical encoder attached to the sample, whose angular resolution was 0.045°. The film was mounted with the *c* axis perpendicular to the sample holder's vertical axis of rotation, which allowed one to change the magnetic field direction in a plane parallel to the *c* axis.

Resistivity was measured using the standard dc four-probe method. The current was applied to the sample in the form of short pulses (of a duration less than 200 ms) in order to reduce Joule heating. A dc current reversal was used to eliminate the thermal emf in the leads. The voltage was measured using a Keithley 2182 Nanovoltmeter in tandem with a Keithley 236 Current Source, with the nanovoltmeter working as the triggering unit. The nanovoltmeter was operated in a mode (known as Delta mode) which allows the measurement and calculation of the voltage from two voltage measurements for two opposite directions of the current. Temperature was monitored by a carbon-glass resistance thermometer and an inductanceless heater, and was controlled to better than ± 10 mK for each single angular sweep in a magnetic field. This was achieved by rotating the sample very slowly in the magnetic field in order to reduce variations in the emf in the heater which could disturb the temperature reading. The term ''resistivity'' is used in this paper to denote the quantity E/J (where E is the electric field and J is the transport current density), and it does not imply an ohmic response.

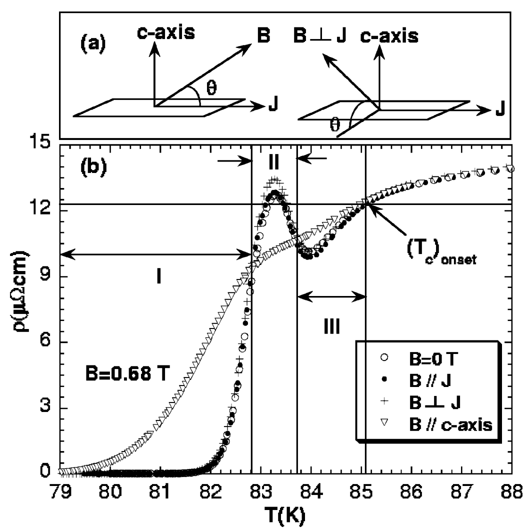

FIG. 1. (a) Two configurations of **B** with respect **J** that were used during the measurements of the angular dependence of resistivity $\rho(\theta)$ in a magnetic field: **B** is rotated in a plane parallel to both **J** and the *c* axis (left side), or **B** is rotated in a plane parallel to the *c* axis but perpendicular to **J** (right side). (b) Temperature dependence of resistivity for YBCO thin film measured in a zero and 0.68 T fields at different orientations. Regions I and III denote the temperature ranges over which $\rho(T)$ is independent of the magnitude of **B** and the angle between **B** and **J** for **B**$\parallel$ *ab* planes. In these regions $\rho(\theta)$ displays a minimum at $\theta=0°$ (**B** parallel to the *ab* planes) [see Figs. 2(a) and 2(c)]. Region II represents the temperature range over which $\rho(T)$ exhibits a peak [of magnitude larger than $\rho(T)$ at the onset T_c], for **B**=0 and for both **B**$\parallel$**J** ($\theta=0°$) and **B**$\perp$ **J** ($\theta=0°$) orientations. Rotating the field from the *ab* planes ($\theta=0°$) toward the *c* axis ($\theta=90°$), leads to an increase in $\rho(T)$ in regions I and III, and to a suppression of the peak in region II.

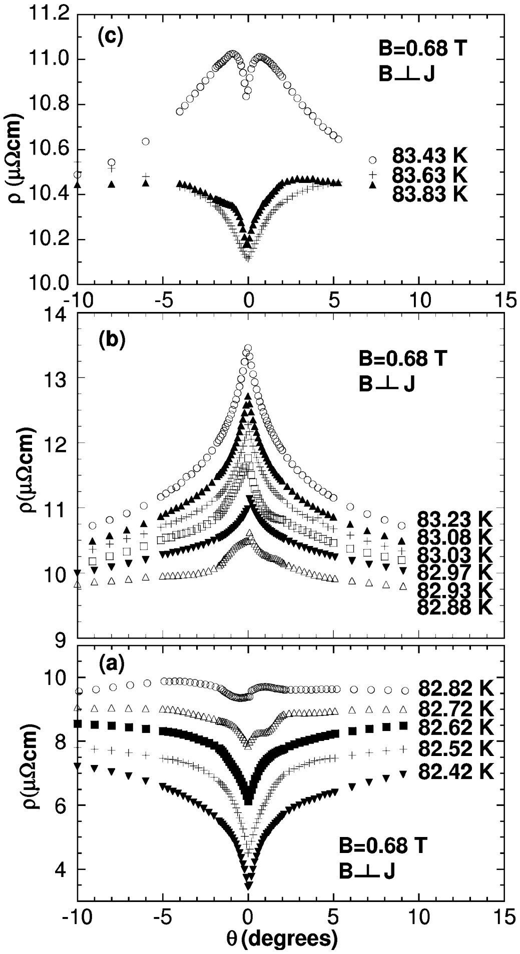

FIG. 2. $\rho(\theta)$ measured in 0.68 T for a temperature range between 82.52 and 83.83 K spanning the three regions I, II, and III. Note the change in $\rho(\theta)$ at $\theta=0°$ from a minimum in region I (a) to a maximum in region II (b) and then back to a minimum in region III (c). In regions I and III, identical behavior of $\rho(\theta)$ has been observed for **B**$\|$**J** and **B**$\perp$ **J** orientations, whereas in region II the magnitude of $\rho(\theta)$ depends on those orientations.

All measurements were carried out with the transport current **J** parallel to the *ab* planes for two different orientations of the magnetic field with respect to the current. For the first one, the field was rotated in a plane perpendicular to the current direction while for the other one the field was rotated in a plane parallel to the current and the *c*-axis directions [see Fig. 1(a)]. All measurements were done in a field cooling regime, with the magnetic field applied to the sample at a temperature above the onset T_c, followed by a slow cooling down to the required temperature of measurement.

III. EXPERIMENTAL RESULTS

A. Temperature dependence of resistivity

The temperature dependence of resistivity ρ was measured over a temperature range of 78–300 K in a zero magnetic field. For a temperature range (78-90 K) close to T_c, ρ was recorded for different orientations of the magnetic field with respect to the direction of the current density **J**. Figure 1(a) shows two possible orientations of the magnetic field **B** with respect to **J** and the *ab* plane of the film. The figure on the left illustrates the case in which the field **B** was rotated in a plane parallel to the direction of **J**, while the one on the right represents the case in which **B** was rotated in a plane perpendicular to **J**. For both orientations **B** was rotated in a plane parallel to the *c* axis. The first configuration is denoted as **B**$\|$**J** and the second one as **B**$\perp$ **J**. Figure 1(b) shows the temperature dependence of resistivity $\rho(T)$ for a temperature range of 79–88 K measured in a zero field and in 0.68 T. The measurements of $\rho(T)$ in the field were carried out for the following orientations of **B** with respect to **J**: **B**$\|$**J** and **B**$\perp$ **J** with **B** parallel to the *ab* plane ($\theta=0°$), and for **B**$\perp$ **J** with **B** parallel to the *c* axis ($\theta=90°$). The onset transition temperature (onset T_c) is defined as the temperature above which the resistivity does not respond to the change in both magnitude and direction of the magnetic field [see Fig. 1(b)]. $\rho(T)$ below the onset T_c could be divided into three regions. Each region is identified according to the response of $\rho(T)$ to the change in the direction of the magnetic field from the *ab* planes ($\theta=0°$) to the *c* axis ($\theta=90°$). Region II represents a temperature range between 82.8 and 83.5 K over which $\rho(T)$ exhibits a peak [of magnitude slightly larger than that of $\rho(T)$ at the onset T_c; see the horizontal line in Fig. 1(b)] in a zero magnetic field, and for **B**$\|$ *ab* planes with **B**$\|$**J** and **B**$\perp$ **J** orientations. Note a clear separation between the peak and the onset T_c. In this region, behavior of $\rho(T)$ changes dramatically upon rotating the field from the *ab* planes to the *c* axis. In regions I and III, $\rho(T)$ was observed to increase when **B** is parallel to the *c* axis, while in region II (the peak region) $\rho(T)$ is completely suppressed by the magnetic field **B**$\|$ *c* axis. For **B**$\|$ *ab* planes, $\rho(T)$ in regions I and III is independent of the magnitude of **B** and the angle between **B** and **J**. However, in region II, $\rho(T)$ is independent of the magnitude of **B** only for **B**$\|$**J** orientation. In this region, $\rho(T)$ was found to decrease with an increasing applied current density **J**. The temperature dependence of resistivity for **B**$\|$*c* axis was measured in different magnetic fields. For fields

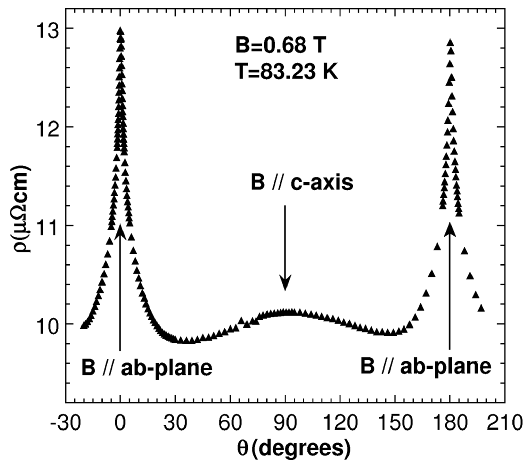

FIG. 3. $\rho(\theta)$ measured in 0.68 T at 83.23 K for an angular range $-30°<\theta<210°$. Note the peaks at $\theta=0°$ and $\theta=180°$ (**B**$\|$ *ab* planes) which are approximately 30% higher than the maximum at $\theta=90°$ (**B**$\|$ *c* axis).

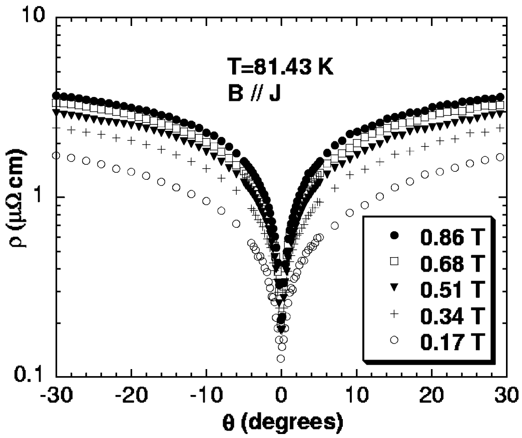

FIG. 4. (a) Angular dependence of resistivity measured at a temperature of 81.43 K (region I) in different fields for **B** close to the *ab* planes. The data reveal a minimum in $\rho(\theta)$ at $\theta=0°$ (**B** parallel to the *ab* planes). The width of the minimum decreases with an in increasing field. An identical behavior has been observed for both **B**⊥ **J** and **B**‖**J** orientations.

above 0.1 T, the peak in region II is completely suppressed. The resistivity between the onset T_c and the room temperature exhibits a linear temperature dependence.

B. Angular dependence of resistivity: Effect of temperature and magnetic field

The angular dependence of resistivity $\rho(\theta)$ was measured in a constant magnetic field at different temperatures in regions I, II, and III, for both **B**‖**J** and **B**⊥ **J** orientations for the angular range from $-20°$ to $+20°$. The measurements revealed minima in $\rho(\theta)$ at $\theta=0°$ in region I and III, and a maximum in region II (see Fig. 2). Figure 2(a) shows $\rho(\theta)$ in region I as a function of temperature between 82.42 and 82.82 K in a magnetic field of 0.68 T. At a temperature of approximately 82.82 K, which corresponds to the border line between region I and II in Fig. 1(b), there is a crossover from a minimum to a peak in $\rho(\theta)$. This peak grows with an increasing temperature reaching a maximum value at 83.23 K [see Fig. 2(b)].

The second crossover from a maximum to minimum can be seen at 83.50 K, which corresponds to the border line between regions II and III in Fig. 1(b). We have measured $\rho(\theta)$ for both **B**⊥ **J** and **B**‖**J** in all three regions. While in regions I and III the minimum in $\rho(\theta)$ is independent of the orientation of **B** with respect to **J** (i.e., for **B**⊥ **J** and **B**‖**J**), in region II the magnitude of the peak depends on these orientations and $\rho(\theta)_{B\perp J}>\rho(\theta)_{B\|J}$.

The measurements of $\rho(\theta)$ over an angular range between $-30°$ and 210° revealed sharp maxima for **B**‖ *ab* planes ($\theta=0°$ and $\theta=180°$) and a smaller broad maximum for **B**‖ *c* axis ($\theta=90°$) (see Fig. 3). $\rho(\theta)$ at $\theta=0°$ and $\theta=180°$ is about 30% larger than that for $\theta=90°$. Moreover $\rho(\theta)$ has minima at $\theta=35°$ and $\theta=145°$ for all fields.

The angular dependence of resistivity $\rho(\theta)$ was also measured at a constant temperature in different magnetic field in regions I, II, and III, for both **B**‖**J** and **B**⊥ **J** orientations and for the angular range between $-20°$ and $+20°$. Figure 4 shows the angular dependence of resistivity, at a temperature of 81.43 K (region I), measured in different magnetic fields for both **B**‖**J** and **B**⊥ **J** orientations. The data for these two orientations are identical, which implies that $\rho(\theta)$ is independent of the angle between **B** and **J**. $\rho(\theta)$ at $\theta=0°$ is almost independent of the magnitude of **B**. The width of this minimum [defined as half width at half minimum (HWHM)] decreases from a HWHM of $=2.3°$ in a field of 0.17 T down to a HWHM of $=2.0°$ in 0.86 T. The depth of the minimum increases with an increasing field. The results of the measurements of $\rho(\theta)$ in region III is identical in all aspects to those obtained in region I.

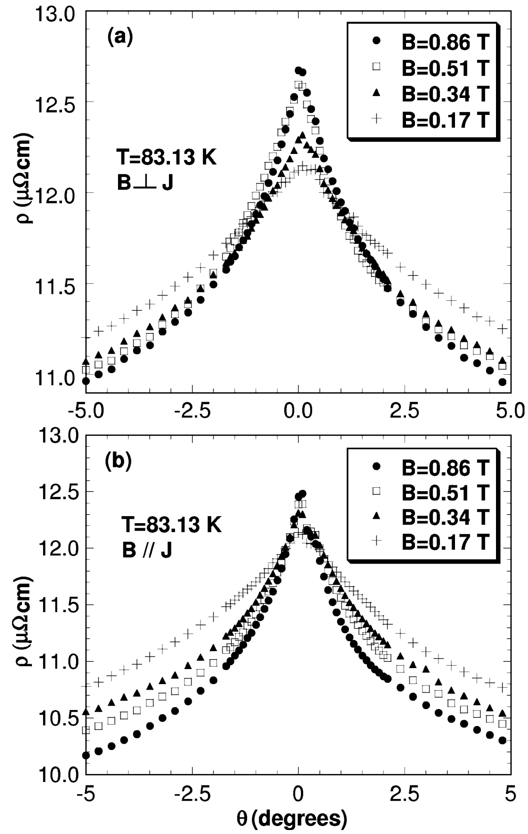

FIG. 5. Angular dependence of resistivity $\rho(\theta)$ for $-5°<\theta<5°$, measured in different applied magnetic fields at a fixed temperature of 83.13 K (region II). (a) $\rho(\theta)$ for **B**⊥ **J** orientation, where $\rho(\theta)$ increases with an increasing **B** for $\theta<1°$ but decreases with an increasing **B** for $\theta>1°$. (b) $\rho(\theta)$ for **B**‖**J** orientation; ρ at $\theta=0°$ is almost independent of **B**. Note that $\rho(\theta)$ decreases with an increasing **B** for $\theta>0.5°$.

Figure 5 presents $\rho(\theta)$ measured at a temperature of 83.13 K (in region II) in different magnetic fields for both **B**⊥ **J** and **B**‖**J** orientations. The width of the peak in $\rho(\theta)$ decreases with an increasing **B** for both **B**⊥ **J** and **B**‖**J** orientations. The magnitude of the peak in $\rho(\theta)$ for **B**‖**J** is almost independent of the magnitude of **B**; however, it increases with **B** for **B**⊥ **J**. A decrease of the peak's width with an increasing magnetic field means that within a certain angular range ($|\theta|>1.5°$ for **B**⊥ **J** and $|\theta|>0.3°$ for **B**‖**J**), $\rho(\theta)$ decreases with an increasing field.

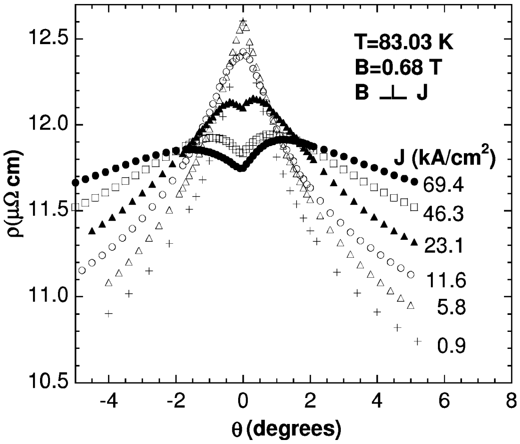

FIG. 6. Angular dependence of resistivity $\rho(\theta)$ measured as a function of applied current density **J** for a field of 0.68 T and a temperature of 83.03 K (region II) . For angles $|\theta|>2°$, $\rho(\theta)$ increases with an increasing **J**, but for small angles $|\theta|<2°$ the opposite happens, where a minimum starts to develop with its width increasing with an increasing applied current.

C. Angular dependence of resistivity: Effect of the applied current

The angular dependence of resistivity was measured also as a function of the applied current density at a constant temperature and magnetic field. Figure 6 presents the measurements of $\rho(\theta)$ in region II for a wide range of applied current density **J**, from 0.9 to 69.4 kA/cm^2, in a field of 0.68 T and at a temperature of 83.03 K. For angles $|\theta|>2°$, $\rho(\theta)$ increases nonlinearly with an increasing **J**, but for small angles $|\theta|<2°$ it decreases with an increasing **J**. In the angular region for $|\theta|<1°$, starting at small current density ($\mathbf{J}\leqslant 11.6$ kA/cm^2), the peak height initially decreases with an increasing current, but for J larger than 23.1 kA/cm^2, a minimum in $\rho(\theta)$ develops. The dependence of $\rho(\theta)$ on **J** is essentially the same for both $\mathbf{B}\|\mathbf{J}$ and $\mathbf{B}\perp\mathbf{J}$ orientations.

Figure 7 shows $\rho(\theta)$ measured in region I for a wide range of **J** in a field of 0.68 T and at a temperature of 81.83 K. Effect of the current on the minimum is different from that observed in region II. The minimum at $\theta=0°$ decreases with an increasing **J**. The dependence of $\rho(\theta)$ on **J** is identical for both $\mathbf{B}\|\mathbf{J}$ and $\mathbf{B}\perp\mathbf{J}$ orientations. Similar dependence of $\rho(\theta)$ on **J** was observed over the temperature range in region III.

IV. DISCUSSION

The experimental data for $\rho(T,B)$ obtained for the underdoped YBCO film are qualitatively similar to those observed before in HTSCs.[1–3] The anomalous resistive peak is located at a temperature approximately 1.8 K lower than the onset T_c. The peak disappears when a magnetic field is applied along the c axis of the film. Also the magnitude of the peak decreases and its position shifts to lower temperatures with an increasing applied transport current. Our measurements of the angular dependence of resistivity in a magnetic field provided very valuable additional information, which allows us to understand better the physics of the anomalous resistivity.

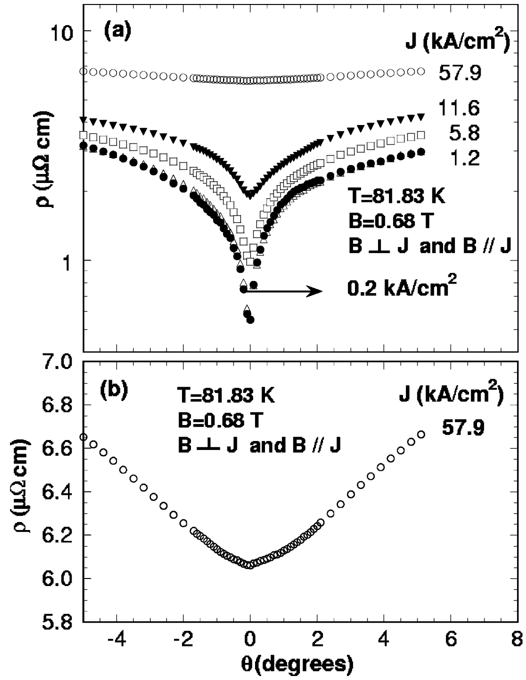

FIG. 7. (a) Angular dependence of resistivity $\rho(\theta)$ measured as a function of an applied current density **J** in a field of 0.68 T and at a temperature of 81.83 K (region I). The sharpness of the minimum at $\theta=0°$ decreases gradually with an increasing J. (b) Expanded view of $\rho(\theta)$ measured at $J=57.9$ kA/cm^2.

The measurements of $\rho(\theta)$ in a magnetic field as a function of temperature revealed sharp minima in resistivity at $\theta=0°$ (**B** parallel to the *ab* planes) at temperatures below and above the resistive peak in $\rho(T)$, and a sharp maximum at $\theta=0°$ at the peak's temperature (see Fig. 2).

The data for $\rho(T)$ and $\rho(\theta)$ were used to distinguish between different interpretations of the resistive anomaly. We considered a two-dimensional resistor model, magnetic flux motion, and thermally activated phase slips.

A. Two-dimensional resistor model

In an inhomogeneous superconductor different parts of the film or the crystal can have slightly different transition temperatures. Vaglio *et al.*[8] and Mosqueira *et al.*[2,17] modeled this type of superconductor as an electrical circuit array of different resistors. The anomalous peak in $\rho(T)$ was produced by solving numerically, through the standard matrix method, the electrical circuit equations using large number of fitting parameters. Mosqueira *et al.* argued that nonuniformly distributed oxygen inhomogeneities (domains with different oxygen content) are responsible for the anomalous resistivity. Differences between samples were taken into account by varying more than seven parameters: the domain size, the spatial distribution of domains, and the differences between transition temperatures of the neighboring domains. These differences were incorporated into the resistor model by varying the magnitudes (as a function of temperature and magnetic field) and the positions of different resistors within the resistor array (different domains were represented by different resistors). The resistor model was first used to analyze

TABLE I. The relative change of resistivity $\Delta\rho/\rho_B=(\rho_P-\rho_B)/\rho_B$, where ρ_P is the peak's resistivity and ρ_B is the resistivity measured in a magnetic field **B*** at the peak's temperature in the absence of the peak. The broadening of the superconducting transition $\Delta T_c(B^*)$ in a magnetic field B^*, at which the peak disappears, is obtained for different superconductors.

Material	$T_c(K)(R=0)$	$\Delta\rho/\rho_B$	$B^*(T)$	$\Delta T_c(B^*)(K)$	Reference
YBCO crystal	90	0.58	1.0	2	17
YBCO crystal	89.3	0.29	0.3	2	2
YBCO film	81.7	0.44	0.08	0.5	this work
BSCCO crystal	93	1.56	0.01	~ 2	3
BSCCO crystal	79	0.41	0.3	~ 5	17
NdCeCuO crystal	23.5	0.28	0.1	~ 4	1
PrCeCuO crystal	20.7	0.16	0.7	<0.5	1
Al thin film strips	1.28	0.17–0.56	0.001	0	4
$(Y_{0.7}Pr_{0.3})$BCO crystal	52.7	0.20	1.0	2	19

the data, measured in a zero magnetic field, for an anomalous resistivity in $\rho(T)$ of Nb-based LTSC films by Vaglio *et al.*[8] Later Mosqueira and co-workers[2,17] used the resistive model to simulate the anomalous peak-resistivity in $\rho_{ab}(T)$ at different magnetic fields for YBCO and BSCCO crystals. As mentioned in the introduction, Browning *et al.*[12] performed two dimensional x-ray diffraction analysis with 10-μm spatial resolution and a few micrometers sampling depth on YBCO crystals with very sharp superconducting transitions. Their data revealed the presence of nonuniformly distributed inhomogeneities of oxygen content $(7-\delta=6.8–7.0)$ across YBCO crystals. A three-dimensional plot of $7-\delta$ versus the position on the crystal's face show domain features a fraction of millimeter in size (see Fig. 12 in Ref. 12). High energy x-ray diffraction, in which the radiation penetrates the entire crystal, was performed recently at Brookhaven National Laboratory and revealed the presence of $(7-\delta)$ nonuniformly distributed inhomogeneities across the crystals.[18] The measurements of the temperature dependence of the resistivity did not show any resistive peak anomalies near T_c in those crystals. In fact, those samples exhibit high $T_c(R=0)\cong 93$ K, sharp superconducting transitions ($\Delta T_c \simeq 0.2–0.3$ K), and low resistivity ($\rho\approx 120\ \mu\Omega$ cm at 300 K). These studies imply that just the presence of nonuniformly distributed T_c inhomogeneities [nonuniformly distributed $(7-\delta)$ domains] is not sufficient to produce the resistive anomalies.

The reduction and subsequently suppression of the resistive peak anomaly with an increasing magnetic field are associated, according to the resistive model,[2,17] with the broadening of the resistive transition. The broadening of the resistive transition as well as the magnitude of the magnetic field required to suppress the anomaly completely is sample dependent (see Table I). Mosqueira *et al.*[17] argued that the resistive model is universal and could be used to explain resistive anomalies in both HTSC and LTSC samples. Unfortunately, it was shown by Santhanam *et al.*[4] that the elimination of the resistive peak by an applied magnetic field in Al thin film strips occurs without any associated broadening of the superconducting transition (see Table I). On the other hand, Moshchalkov *et al.*[5] observed the resistive anomalies in Al thin film 1D strips (wires) of dimensions less than the Ginzburg-Landau coherence length close to the onset T_c. Their studies implied that inhomogeneities are not responsible for the presence of the resistive peaks in Al quasi-1D wires.

The resistive model was applied by Mosquiera and co-workers[2,17] to perform computer simulations of the resistive anomalies in YBCO and BSCCO crystals subjected to a magnetic field which was applied in a direction perpendicular and parallel to the *ab* planes. The experimental data show the broadening of the resistive transition for both field orientations and for both YBCO and BSCCO. In order to obtain a good fit to the data for BSCCO, the authors had to assume an unrealistic value for the intrinsic anisotropy factor ($\gamma=10^3$) which is two orders of magnitude less than the accepted value ($\gamma=10^5$). It seems that the resistive model should not be applied to cases in which the transition width is not sensitive to an applied magnetic field, like the example of the highly anisotropic BSCCO with a magnetic field applied parallel to the CuO_2 layers. In the case of YBCO film, as discussed in Sec. IV B, the rotation of the magnetic field in the *ab* planes from $\mathbf{B}\perp\mathbf{J}$ to $\mathbf{B}\|\mathbf{J}$ orientations, reduces the magnitude of the anomalous peak in $\rho(T)$ without any observable broadening of the transition width, indicating that the resistive model is not adequate to explain all the phenomena observed in our case. According to our interpretation, nonuniformly distributed T_c inhomogeneities introduced by the resistive model are necessary but not sufficient conditions for the resistive anomalies to occur.

B. Flux motion

In order to find the contribution of the magnetic flux motion to the observed resistive anomaly, we performed the measurements of $\rho(T)$ and $\rho(\theta)$ for two different orientations of the current relative to the magnetic field, i.e., for $\mathbf{B}\perp\mathbf{J}$ and $\mathbf{B}\|\mathbf{J}$ orientations (see Fig. 1). The magnitude of the peak in $\rho(T)$ (region II in Fig. 1) increases when the field is parallel to the *ab* planes and perpendicular to the current i.e., for $\mathbf{B}\perp\mathbf{J}$ (compared to the case for $\mathbf{B}\|\mathbf{J}$). This situation corresponds to the maximum Lorenz force acting on the flux lines along the *ab* planes. The angular dependence of ρ in a magnetic field (Fig. 2) reveals a maximum in region II, but sharp minima at temperatures below and above the peak (regions I and III in Fig. 1). A very sharp minimum in $\rho(\theta)$ at $\theta=0°$ ($\mathbf{B}\parallel ab$ planes) was seen previously in a YBCO single crystal by Kwok *et al.*[20] and interpreted as due to the lock-in transition of the flux lines trapped between the planes. For a system of weakly coupled CuO_2 layers one expects a maximum resistive dissipation for $\mathbf{B}\parallel c$ axis and a minimum for $\mathbf{B}\parallel ab$ planes. An increase in $\rho(\theta)$ when the field is rotated from the *ab* planes to the *c* axis is normally attributed to the intrinsic anisotropy of the material. We found that the minima in $\rho(\theta)$ at $\theta=0°$ (regions I and III) are independent of the orientation of the current relative to $\mathbf{B}$ (see Fig. 4), suggesting a very strong flux lock-in mechanism when $\mathbf{B}$ is parallel to the *ab* planes. For $\theta>0°$ resistivity could arise via the nucleation and motion of kinks along the vortex lines.[20] In this case, one could also describe the tilted vortex line as a combination of Josephson strings aligned along the *ab* planes and mobile pancakes (vortex segments along the *c* axis). If the coupling between the pancake vortices is weak, the Lorenz force acting on these vortices, and consequently their motion, should be independent of the direction of the transport current in the *ab* planes. The measurement of the minimum in $\rho(\theta)$ also revealed an increase of the resistivity with an increasing transport current in the *ab* planes (Fig. 7), which is independent of the orientation of the current relative to $\mathbf{B}$. This result suggests that the motion of the pancake-vortices in the *ab* planes is responsible for the observed increase of $\rho(\theta)$ for $\theta>0°$ in regions I and III. The maximum in $\rho(\theta)$ at $\theta=0°$ at temperatures corresponding to region II in $\rho(T)$ (Fig. 5) depends on the orientation of the current relative to $\mathbf{B}$. For $\mathbf{B}\perp\mathbf{J}$ orientation, the maximum is higher than that measured for $\mathbf{B}\parallel\mathbf{J}$ orientation. This behavior is different from that observed in regions I and III, and therefore it provides additional argument that the peak in $\rho(T)$ cannot be explained by the 2D resistor model alone. It also suggests that the unknown dissipation in region II weakens flux lock-in between the planes. Subtracting the maximum in $\rho(\theta)$ at $\theta=0°$ for $\mathbf{B}\parallel\mathbf{J}$ from that measured for $\mathbf{B}\perp\mathbf{J}$ (see Fig. 8) gives $\rho(\theta)$ with a minimum similar to those observed in regions I and III, which are caused by flux motion.

The measurement of the maxima in $\rho(\theta)$ at $\theta=0°$, as a function of magnetic field for $\mathbf{B}\parallel\mathbf{J}$ and $\mathbf{B}\perp\mathbf{J}$ orientations, shows that the maxima become sharper (i.e their width decreases) with an increasing magnetic field. For both $\mathbf{B}\parallel\mathbf{J}$ and $\mathbf{B}\perp\mathbf{J}$ orientations, and for $\theta>1.5°$, the resistivity at a fixed θ decreases with an increasing field (Fig. 5). On the other hand, the maximum in $\rho(\theta)$ at $\theta=0°$ also decreases with an increasing transport current (Fig. 6). This reduction in resistivity cannot be explained by the flux motion. Chaparala *et al.*[21] observed a small maximum in $\rho(\theta)$, when the magnetic field was oriented parallel to the *ab* planes in Tl (2212, 1223) and BSCCO(2212) crystals. The authors did not present any data for the corresponding temperature dependence of the resistivity. The maximum in resistivity was attributed to the formation and motion of the *c*-axis-oriented vortex-antivortex segments of the flux lines parallel to the *ab* planes. They assumed that the maximum is created as a result of the interplay between the density n_s and the velocity v_s of the vortex-antivortex segments. The resistive potential

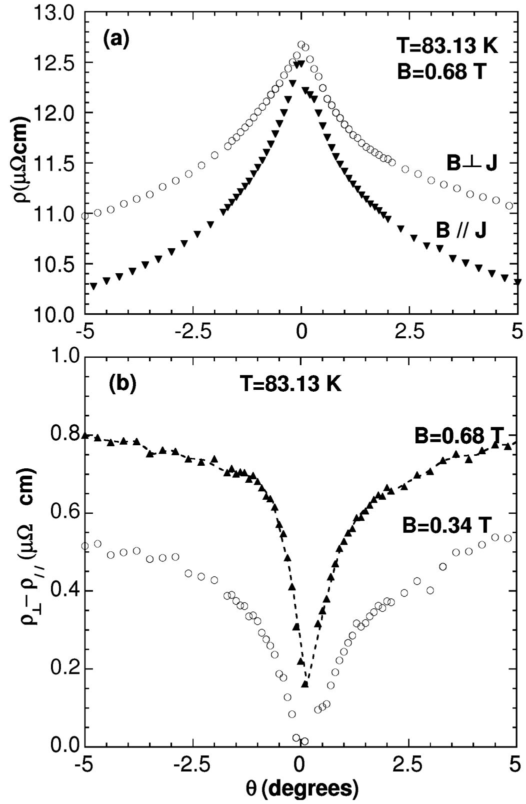

FIG. 8. (a) Comparison between $\rho(\theta)$ measured for $\mathbf{B}\perp\mathbf{J}$ and $\mathbf{B}\parallel\mathbf{J}$ orientations in 0.68 T at 83.13 K. (b) The difference $\Delta\rho(\theta)$ between the peaks in $\rho(\theta)$ for $\mathbf{B}\perp\mathbf{J}$ and $\mathbf{B}\parallel\mathbf{J}$ orientations measured in 0.34 and 0.68 T.

difference V is proportional to the product of these quantities. According to the experimental observation $V\propto(n_s v_s)_{\theta=0°}$ is larger than $V\propto(n_s v_s)_{\theta>0°}$. Chaparala *et al.*[21] argued that, at $\theta=0°$, in spite of the small density of the vortices, $n_s v_s$ is large because of the high velocity of the newly created vortex-antivortex pairs. At $\theta>0°$, n_s is large but v_s is small, so $(n_s v_s)_{\theta=0°}>(n_s v_s)_{\theta>0°}$. According to this interpretation, increasing the applied transport current should increase the Lorenz force on these pairs, and consequently increase their velocity. This leads to an increase in the resistive dissipation and to the growth of the maximum in $\rho(\theta)$ at $\theta=0°$ with an increasing current. Our data revealed a reduction of the maximum in $\rho(\theta)$ at $\theta=0°$ with an increasing current (see Fig. 6), which eliminates the vortex-antivortex model as a possible explanation of the resistive anomaly. The absolute values of the resistivity in the peak observed on $\rho(T)$ curve is slightly higher than the resistivity at the onset T_c (85 K), defined as the temperature above which the resistivity is independent of the magnitude and direction of the applied magnetic field [see the horizontal line in Fig. 1(b)]. The resistive dissipation due to a vortex motion can reduce the critical current density to zero, reaching the normal state resistivity, but it cannot exceed this value.

C. Phase-slip model

The discussion of the resistive-peak anomaly in Sec. IV A and B indicates that 2D resistor and flux motion models alone cannot fully account for the origin of this phenomenon. Regarding LTSCs, Moshchalkov *et al.*[5] argued that the resistive anomaly, seen in 1D Al wires, originate from thermally activated phase slips, and the observed resistive peak at the onset T_c is the result of the phase-slip resistivity and the normal state resistivity acting in series. Observation of the similar resistive peak anomaly in LTSC disordered films implies that, in some disordered systems, a filamentary flow of the transport current could occur through 1D constrictions (channels). We believe that this could also happen in HTSC samples. Browning *et al.*[12] revealed that in spite of a large variation of the oxygen content ($7-\delta=6.8$–7.0) measured across YBCO crystals, they still display sharp superconducting transitions (~ 0.2 K), high T_c, and low resistivity. This implies filamentary flow of the current in the samples. However, the resistive peak anomaly is absent in the samples which could mean that the filamentary flow alone is not sufficient to produce the resistive anomalies. We conclude by analogy to the case of LTSC disordered films that thermally activated phase slips could produce such an anomaly if the filamentary flow of the current occurs through 1D constrictions. This could happen more likely in underdoped HTSC samples due to phase-separation-induced disorder. It should also be noted that our data show all qualitative basic characteristics expected by the LA-MH phase-slip model.[11,10] According to this model phase-slip events lead to the appearance of a resistance in 1D superconducting wires below T_c. During a phase slip event, thermal fluctuations reduce the superconducting order parameter, defined as $\psi(x) = |\psi(x)|e^{i\phi(x)}$, where $\phi(x)$ is the phase, to zero at some point along the wire momentarily disconnecting the phase coherence. This allows the relative phase across the wire to slip by 2π [before $\phi(x)$ recovers its finite value], resulting in a resistive voltage.

For a 1D thin wire with a transverse dimension $d \ll \xi$ and $d \ll \lambda$, the LA-MH theory predicts that the appearance of a resistance in the superconducting state is mainly determined by thermally activated phase slips events as the system is passing over a free energy barrier ΔF_0 (the difference in free energy between the normal and superconducting states) proportional to the cross-sectional area A of the wire,

$$\Delta F_0 = \frac{8\sqrt{2}}{3}[A\xi(T)H_c^2(T)/8\pi], \tag{1}$$

where $H_c(T)$ is the thermodynamic critical field.

In the absence of the current, phase slips by $\pm 2\pi$ are equally likely, and this results in a fluctuating noise voltage with a zero net dc component. The result of the application of a current to the wire is to make the phase jumps more probable in one direction than in the other. The different jump rates arise from a difference δF in the energy barrier for jumps in two directions, and this difference stems from the electric work $\int IVdt$ done in the process. For a phase slip of 2π, the energy difference is $\delta F = \Delta F_+ - \Delta F_- = (h/2e)I_s = \phi_0 I_s$, where $\phi_0 = h/2e$ is the superconducting flux quantum. $\delta F = \phi_0 I_s$ should be larger than the thermal energy $k_B T$, which defines the characteristic current $I_1 = k_B T/\phi_0$, above which most phase slips go in the driven direction and the resistance is nonlinear.[22] I_1 sets a lower limit on the applied current I_s. The upper limit is set by the critical current I_c which is the mean-field critical current given by $I_c = \pi\sqrt{\frac{2}{3}}(\Delta F_0/\phi_0)$, and

$$I_1 = \frac{k_B T}{\phi_0} < I_s < I_c. \tag{2}$$

The average voltage V_s arising from the phase slip events is determined by the number of these events in the sample [$N(T) = L/\xi(T)$, where L is the length of the wire], a characteristic time $\tau(T)$, Boltzmann factor $\exp(-\Delta F(T)/k_B T)$, and the factor $\sinh(I_s\phi_0/2k_B T)$ derived from the difference δF in the energy barrier for the $+2\pi$ and -2π phase jumps.[5,22] V_s is determined by

$$V_s = 2\phi_0 \Omega(I_s, T)\exp\left[-\frac{\Delta F(T)}{k_B T}\right]\sinh\left(\frac{I_s}{2I_1}\right), \tag{3}$$

where $\Delta F(T) = \Delta F_0(T) + (\frac{2}{3})^{1/2} I_s^2 k_B T/3\pi I_1 I_c$ and $\Omega(I_s, T)$ is an attempt frequency which can be approximated as

$$\Omega(I_s, T) = \frac{N(T)}{\tau(T)}\sqrt{\frac{\Delta F_0}{k_B T}}\left(1 - \frac{2I_s}{3I_c}\right)^{15/4}. \tag{4}$$

It is very important to emphasize the fact that the energy being supplied during the occurrence of these phase slips at a rate of IV, is dissipated as heat rather than converted into the kinetic energy of supercurrent, which would otherwise soon exceed the condensation energy.[22]

The magnetic field dependence of the phase-slip event does not appear explicitly in Eq. (3); however, its effect on the phase-slip voltage appears through the dependence of the critical current I_c on B [$I_c \propto (1/B)$]. Phase-slip resistivity is present over a range of the applied current I_s between I_1 and I_c, according to Eq. (2). The applied current I_s per 1D current channel should be larger than $I_1 = k_B T/\phi_0$. If I_s is too close to I_c, phase-slip events are less likely to occur. Also, reducing, I_c while keeping I_s fixed, leads to the reduction of the phase-slip events and consequently the voltage V_s. For an anisotropic superconductor, increasing the magnitude of the c-axis component of **B** by increasing the angle θ and/or the magnitude of **B**, reduces I_c.

The angular dependence of resistivity in a magnetic field measured over a temperature range between 82 and 84 K (Fig. 2) points out different origin of resistivity in the peak in $\rho(T)$ (Fig. 1), in comparison to that at temperatures below and above the peak. Therefore, $\rho(T)$ could be treated as a superposition of the peak and the normal resistivity near the transition, which increases almost linearly with temperature between $T_c(R=0) \simeq 82$ K and the onset $T_c \simeq 85$ K. We considered the possibility that the resistive peak originates from thermally activated phase slips and attempted to perform numerical calculations of the phase-slip resistivity using the modified LA-MH theory. We assumed that in an underdoped HTSC sample the current flows through n parallel superconducting filaments of length 0.4 mm (which is the distance between the voltage contacts). The width w (in the ab planes) and the thickness t (along the c axis) of a filament were chosen to be 2.0 and 1.0 nm, respectively. These values are much smaller than the coherence length in the *ab* planes and along the *c* axis at temperatures close to T_c, and therefore the filaments can be treated as 1D wires. In the system of n parallel superconducting filaments, one could expect that the phase-slip event occurring in a filament would affect the superconducting state of the neighboring filaments, because the coherence length at temperatures close to T_c is much larger than the spacing between the filaments. On the other hand, in an underdoped system, one could also expect that along each filament the superconducting regions are interrupted by segments of normal resistance R_N, so that the total resistance of the filament R_f is the sum of the phase-slip resistance and the normal state resistance acting in series: $R_f = n_s R_s + R_N$, where n_s is the number of the superconducting segments of an average length l_s and an average phase-slip resistance R_s. The arguments presented above suggest that for a system of n parallel filaments, the formula for the condensation energy ΔF_0 [Eq. (1)] for phase-slip events in a 1D wire should be modified to reflect the phase-slip events in the whole system of $n \cdot \overline{n_s}$ segments. We assumed ΔF_0 in the form

$$\Delta F_0 = \frac{8\sqrt{2}}{3}[A\xi_{ab}(T)H_c^2(T)/8\pi]\cdot n \cdot \overline{n_s}, \qquad (5)$$

where n is the total number of filaments, and $\overline{n_s}$ is the average number of superconducting segments per filaments (the average number of phase-slip centers per filament). The Ginzburg-Landau expression for $H_c(T) = H_c(0)(1 - T/T_c) = H_{c2}(0)(1 - T/T_c)/\sqrt{2}\kappa$, and $\xi_{ab}(T) = \xi_{ab}(0)/(1 - T/T_c)^{1/2}$ close to T_c were used. The phase-slip voltage V_s was calculated using Eq. (3) and the modified attempt frequency $\Omega(I_s, T)$. The number of the phase-slip events in a segment was given by $N(T) = l_s/\xi_{ab}(T)\tau(T) = \gamma L/\xi_{ab}(T)\tau(T)$, where $\gamma = l_s/L$. γ and $\overline{n_s}$ were treated as the fitting parameters.

The result of the calculation of the phase-slip resistivity $\rho(T)$ (phase-slip resistance $R_s = V_s/I_s$) is shown in Fig. 9(b) for the following parameters: $I_s = 1\,\mu A$, $H_{c2ab}(0) = 674$ T,[23] $\xi_{ab}(0) = 2.4$ nm,[23] $\kappa = [\lambda_{ab}(0)/\xi_{ab}(0)] = 58$,[23] $n = 4.5 \times 10^6$, $T_c = 84.4$ K, $L = 0.4$ mm, $A = (2\text{nm}) \times (1\text{nm})$, $\gamma = 0.067$, and $\overline{n_s} = 8$. According to Fig. 1, the peak does not contribute to $\rho(T)$ at temperatures above approximately 84 K, which corresponds to $V_s = 0$. The LA-MH theory does not apply at temperatures very close to T_c because of the condition for the applied current I_s which must be smaller than I_c [Eq. (2)]. Therefore in the calculation we used T_c about 0.4 K higher. A good agreement between the experimental data and the calculated resistivity versus temperature was obtained (see Fig. 9).

The experimental data show that the reduction of the resistive peak magnitude in $\rho(T)$ and the width of the peak in $\rho(\theta)$ at $\theta = 0°$ occurs when the magnetic field direction is rotated from the *ab* planes ($\theta = 0°$) toward the *c* axis ($\theta = 90°$) (see Fig. 1). When B is rotated from $\theta = 0°$ position, its *c* axis component $B \sin\theta$ increases, and the critical current I_c in the *ab* planes decreases. The resistive peaks in $\rho(T)$ and $\rho(\theta)$ at $\theta = 0°$ also decrease in magnitude with an increasing applied transport current I_s (see Fig. 7). We verified, using numerical calculations that according to the LA-MH theory, that the phase-slip voltage decreases with an increasing I_s and a decreasing I_c in the limit of very small currents (see Fig. 10).

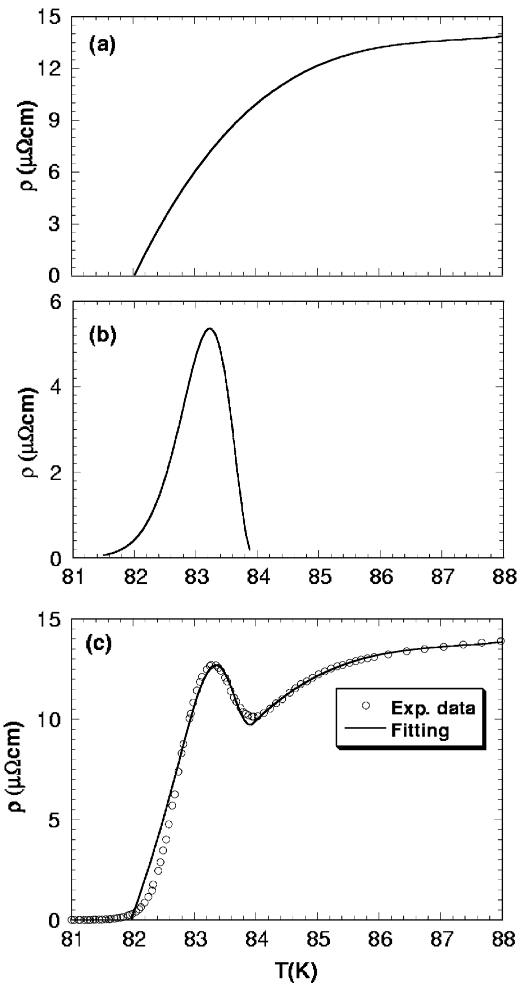

FIG. 9. (a) The assumed normal state resistivity without phase-slip resistivity contribution in a zero magnetic field. (b) The calculated phase-slip resistivity. (c) The fitting to the experimental data obtained by superposition of the normal state resistivity in (a) and the calculated phase-slip resistivity in (b).

V. SUMMARY AND CONCLUSIONS

We investigated the resistive peak anomaly in underdoped YBCO, which was observed in both the temperature dependence of resistivity $\rho(T)$ and the angular dependence of resistivity $\rho(\theta)$ in an applied magnetic field **B**. The resistive peak anomaly in $\rho(T)$ decreases with an increasing **B** (applied parallel to the *c* axis) and with an increasing applied transport current I_s. On the other hand, the width of the resistive peak in $\rho(\theta)$ at $\theta = 0°$ decreases with an increasing **B**, and its magnitude decreases with an increasing I_s. The resistive peak anomaly in $\rho(T)$ and its dependence on **B** and I_s show striking qualitative similarities to those exhibited by LTSC wires, and some LTSC thin films and HTSC crystals.

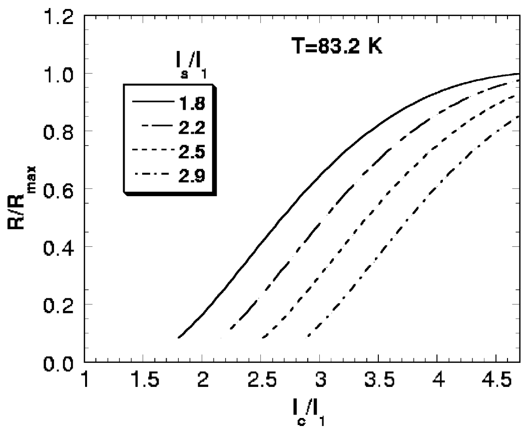

FIG. 10. The calculated phase-slip resistivity as a function of the normalized critical current (I_c/I_1) at different applied currents I_s.

The YBCO film that we analyzed has a resistivity much lower than YBCO crystals studied by Mosqueira *et al.*,[2] suggesting that the resistive peak anomaly is not directly related to the absolute value of the normal state resistivity. The anomaly can not be explained by the *c*-axis misalignments, since they would eliminate the sharp minimum in $\rho(\theta)$ at $\theta = 0°$ ($\mathbf{B} \| ab$ planes) observed in regions I and III.

We analyzed the data in terms of three different models that were developed in the past to explain the resistive anomalies. The 2D resistor model and the flux motion models are inadequate to explain fully our data, including the dependence on a magnetic field and an applied transport current. The phase-slip (LA-MH) model provides the best qualitative and quantitative description of the observed resistive anomalies and their behavior as a function of temperature T, magnetic field $\mathbf{B}$, the angle between $\mathbf{B}$ and the ab planes, and the applied transport current I_s. This model can be applied under the assumption that the current flows through 1D filaments.

ACKNOWLEDGMENTS

This work was supported by a grant from the Natural Sciences and Engineering Research Council of Canada (NSERC). We are grateful to M. Denhoff for supplying us with YBCO thin films. We benefited from discussions with W.-K. Kwok, V. Vinokur, and G. Crabtree.

*Electronic address: mabdel@phys.ualberta.ca
†Electronic address: jung@phys.ualberta.ca

[1] M. A. Crusellas, J. Fontcuberta, and S. Pinol, Phys. Rev. B **46**, 14 089 (1992); L. Fabrega, M. A. Crusellas, J. Fontcuberta, X. Obradors, S. Pinol, C. J. Van der Beek, P. H. Kes, T. Grenet, and J. Beille, Physica C **185-189**, 1913 (1991).
[2] J. Mosqueira, A. Pomar, A. Diaz, J. A. Veira, and F. Vidal, Physica C **225**, 34 (1994).
[3] S. H. Han, Y. Zhao, G. D. Gu, G. J. Russell, and N. Koshizuka, Adv. Supercond. **8**, 109 (1996).
[4] P. Santhanam, C. C. Chi, S. J. Wind, M. J. Brady, and J. J. Bucchignano, Phys. Rev. Lett. **66**, 2254 (1991).
[5] V. V. Moshchalkov, L. Gielen, G. Neuttiens, C. Van Haesendonck, and Y. Bruynseraede, Phys. Rev. B **49**, 15 412 (1994).
[6] Y. K. Kwong, K. Lin, P. J. Hakonen, M. S. Isaacson, and J. M. Parpia, Phys. Rev. B **44**, 462 (1991).
[7] E. Spahn and K. Keck, Solid State Commun. **78**, 69 (1991).
[8] R. Vaglio, C. Attanasio, L. Maritato, and A. Ruosi, Phys. Rev. B **47**, 15 302 (1993).
[9] A. Nordstrom and O. Rapp, Phys. Rev. B **45**, 12 577 (1992).
[10] J. S. Langer and V. Ambegaokar, Phys. Rev. **164**, 498 (1967).
[11] D. E. McCumber and B. I. Halperin, Phys. Rev. B **1**, 1054 (1970).
[12] V. M. Browning, E. F. Skelton, M. S. Osofsky, S. B. Qadri, J. Z. Hu, L. W. Finger, and P. Caubet, Phys. Rev. B **56**, 2860 (1997).
[13] N. H. Andersen, B. Lebech, and H. F. Poulsen, Physica C **172**, 31 (1990).
[14] M. M. Abdelhadi and J. Jung (unpublished).
[15] J. D. Jorgensen, ANL (private communication).
[16] P. G. Radaelli, C. U. Segre, D. G. Hinks, and J. D. Jorgensen, Phys. Rev. B **45**, 4923 (1992).
[17] J. Mosqueira, S. R. Curras, M. V. Ramallo, Th. Siebold, C. Torron, J. A. Campa, I. Rasines, and F. Vidal, Supercond. Sci. Technol. **11**, 821 (1998).
[18] M. S. Osofsky, NRL (private communication).
[19] A. K. Pradhan, S. J. Hazell, J. W. Hodby, C. Chen, A. J. S. Chowdhury, and B. M. Wanklyn, Solid State Commun. **88**, 723 (1993).
[20] W. K. Kwok, U. Welp, V. M. Vinokur, S. Fleshler, J. Downey, and G. W. Crabtree, Phys. Rev. Lett. **67**, 390 (1991).
[21] M. Chaparala, O. H. Chung, Z. F. Ren, M. White, P. Coppens, J. H. Wang, A. P. Hope, and M. J. Naughton, Phys. Rev. B **53**, 5818 (1996).
[22] M. Tinkham, *Introduction to Superconductivity* (McGraw-Hill, New York, 1996).
[23] U. Welp, W. K. Kwok, G. W. Crabtree, K. G. Vandervoort, and J. Z. Liu, Phys. Rev. Lett. **62**, 1908 (1989).